Unveiling Surface Dynamics: In-Situ Oxidation of Defective WS_2

Supplementary Information

Daria Kieczka[a,b], Fabio Bussolotti[b,c], Thathsara D Maddumapatabandi[b,c], Michel Bosman[b,d], Alexander Shluger[a], Anna Regoutz[e], and Kuan Eng Johnson Goh[b,c,f,g]

[a]Department of Physics and Astronomy and London Centre for Nanotechnology, University College London, Gower Street, London WC1E 6BT, United Kingdom

[b]Institute of Materials Research and Engineering (IMRE), Agency for Science Technology and Research (A*STAR), 2 Fusionopolis Way, Innovis #08-03, Singapore 138634, Republic of Singapore

[c]Quantum Innovation Centre (Q.InC), Agency for Science Technology and Research (A*STAR),, 2 Fusionopolis Way, Innovis #08-03, Singapore 138634, Republic of Singapore

[d]Department of Materials Science and Engineering, National University of Singapore, 9 Engineering Drive 1, Singapore 117575, Singapore

[e]Department of Chemistry, University College London, 20 Gordon Street, London, WC1H 0AJ, UK

[f]Division of Physics and Applied Physics, School of Physical and Mathematical Sciences, Nanyang Technological University, 50 Nanyang Avenue 639798, Singapore

[g]Department of Physics, National University of Singapore, 2 Science Drive 3, Singapore 117551, Singapore

List of Figures

List of Tables

1 SM Figures

Table 1: Defect formation energies and binding energies for various cluster sizes in WS_2, calculated using $E_{\text{gain}}/N = \sum_N E_N^f - E_{\text{complex}}^f$. Larger clusters show increased binding energies, indicating enhanced defect stability. Up to 3 S vacancies have been calculated using a $6 \times 6 \times 2$ supercell and $9 \times 9 \times 2$ supercell for larger clusters.

Cluster size	Defect formation energy (eV)	Binding energy of cluster per vacancy (eV)
1	3.16	0.00
2	6.31	-0.01
3 (Line)	9.42	0.00
3 (V shape)	9.48	-0.02
3 (Triangle)	9.79	-0.12
4	13.17	-0.13
5	16.54	-0.15
6	20.03	-0.18
7	23.78	-0.24

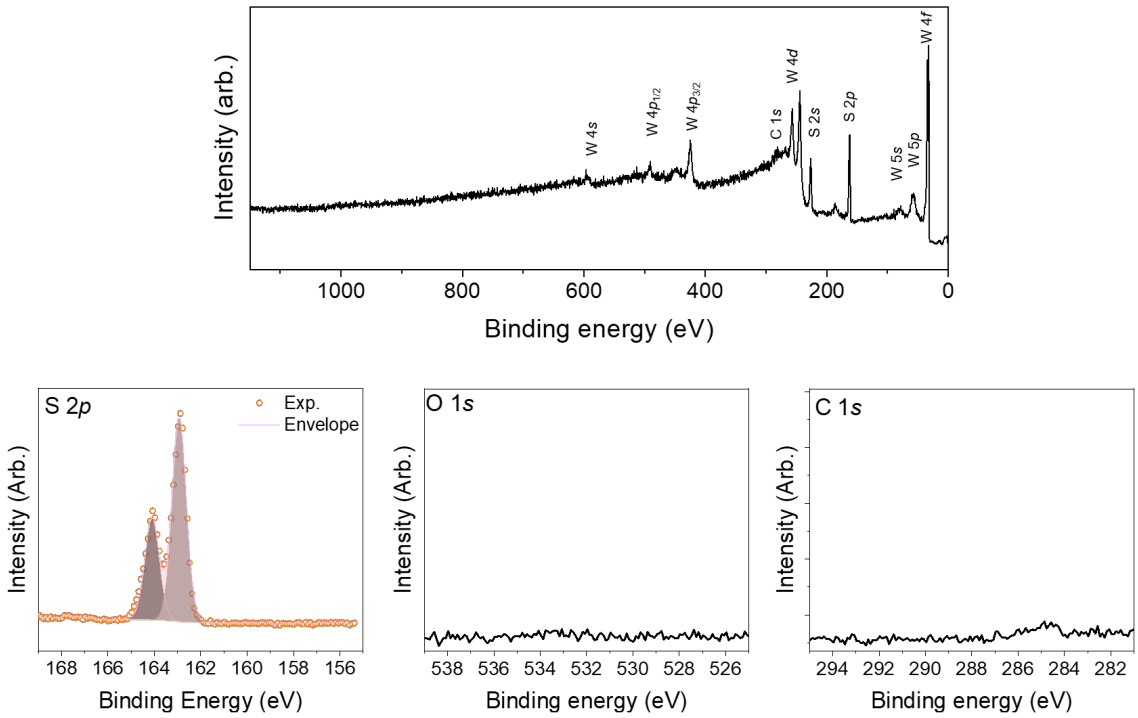

Figure S1: XPS survey spectrum of a freshly cleaved WS_2 surface. The spectrum reveals the presence of mainly W and S. The core level spectra of S 2*p*, O 1*s*, and C 1*s* are also shown. There is a small amount of C likely due to residual contamination from the UHV chamber or the scotch tape used to exfoliate the surface.

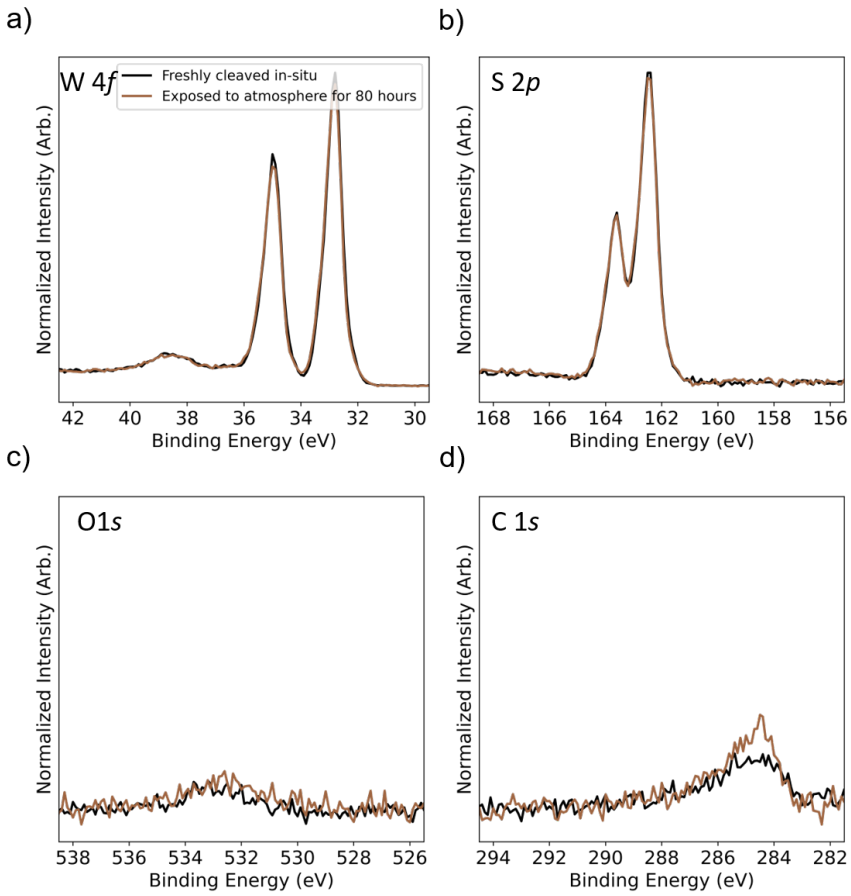

Figure S2: Core levels of the freshly cleaved WS_2 surface after 80 hours of exposure to ambient laboratory atmosphere. No significant changes are observed in the W 4*f* core level, indicating negligible oxidation within this timeframe. However, there is an increase in the intensities of O 1*s* and C 1*s*, suggestig physisorption of O and C species on the surface. (a) W 4*f*, (b) S 2*p*, (c) O 1*s*, (d) C 1*s* spectra, all normalized to the total area of W 4*f*.

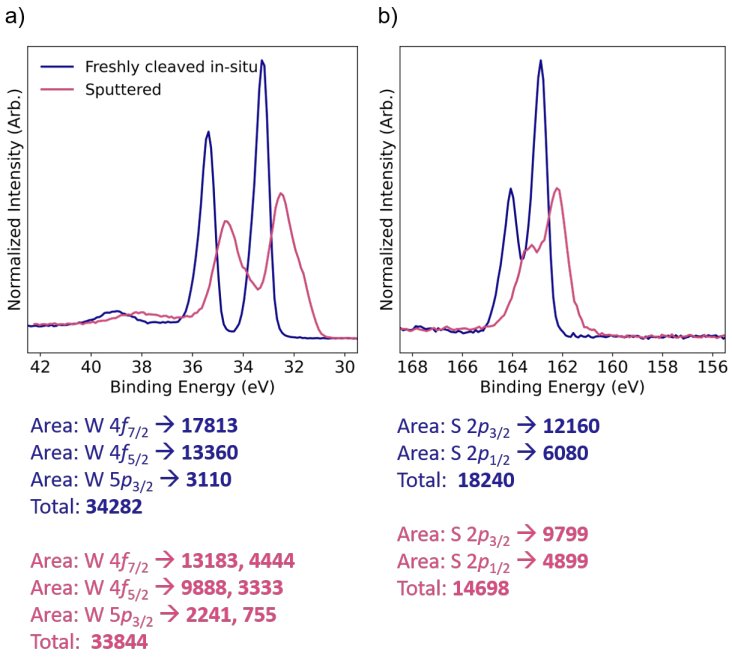

Figure S3: W 4*f* and S 2*p* core level spectra before and after sputtering of the WS_2 surface. (a) The W 4*f* area remains largely unchanged. (b) A 20% decrease in the S 2*p* area post-sputtering (from 18240 to 14698), indicating S removal. Confirming that the sputtering process primarily creates S vacancies rather than W defects.

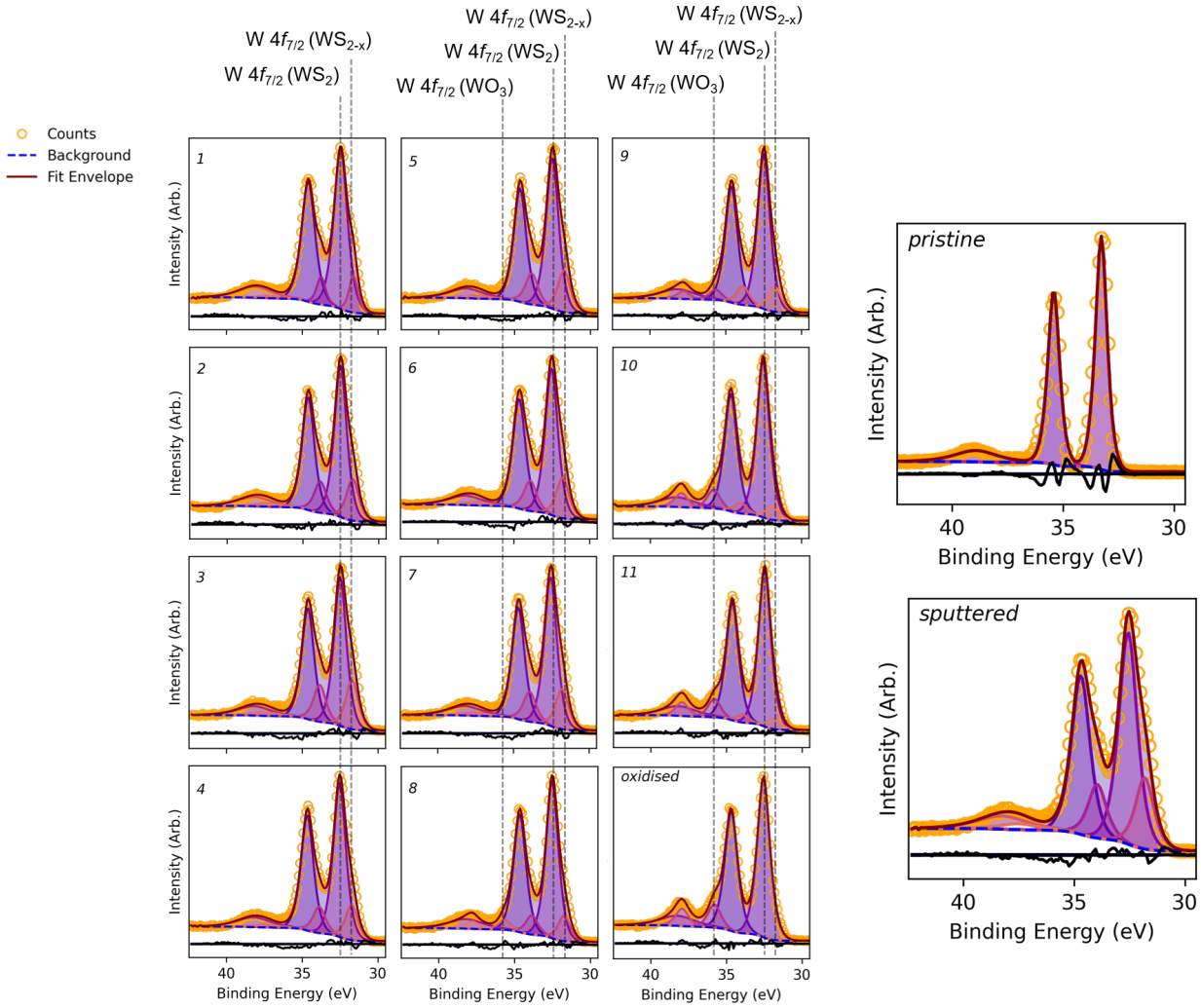

Figure S4: Fits of the W 4*f* core level spectra corresponding to various chemical environments. Residuals (in black line) for each fit are plotted below, showing good agreement with experimental data. The fits help to deconvolute the contributions from different oxidation states of W.

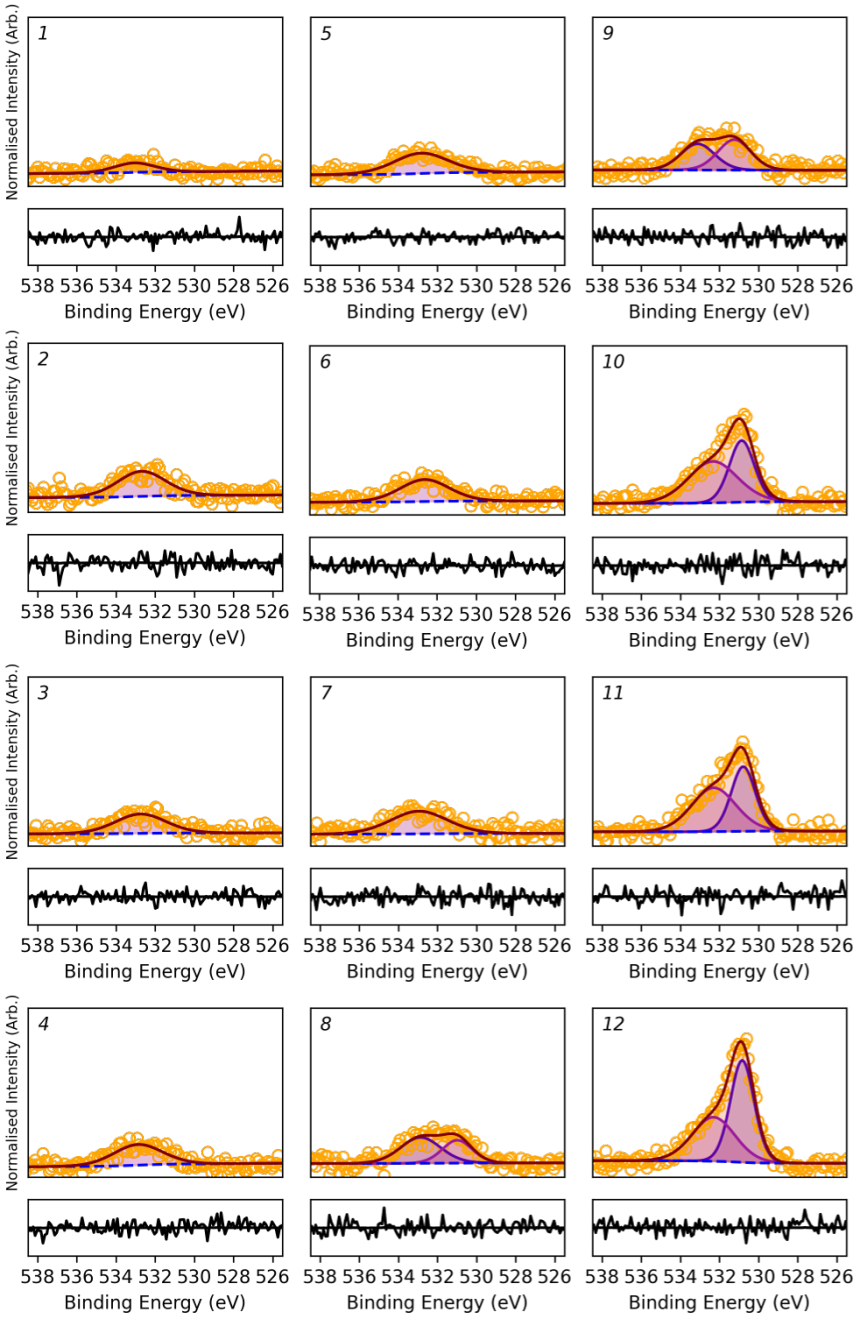

Figure S5: Fits of the O 1*s* core level spectra and residuals, illustrating the evolution of the O signal as oxidation progresses. The increase in peak intensity at lower binding energies suggests the chemisorption of oxygen into the WS_2 lattice, forming tungsten oxides.

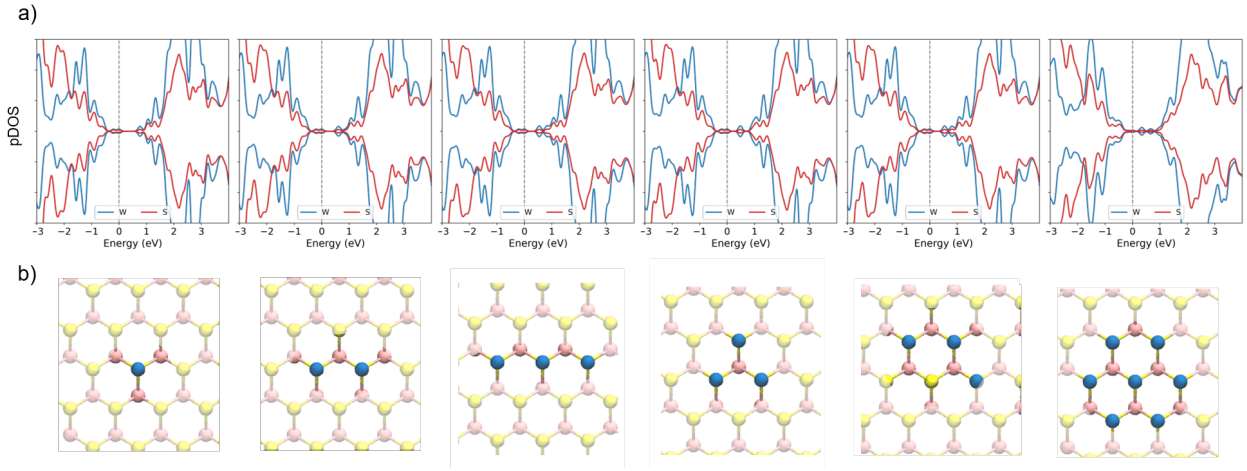

Figure S6: Calculated defect states and corresponding structural models of S vacancies in WS_2. (a) Projected density of states (pDOS) showing the appearance of empty in-gap states near the conduction band (CB), with the number of defect states increasing as the vacancy cluster size grows. (b) Structural models for different vacancy configurations.

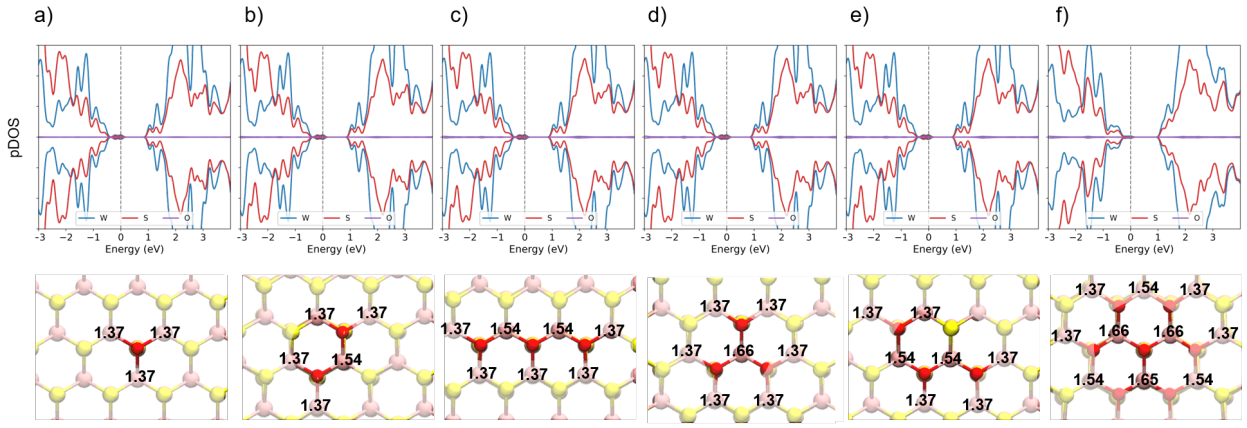

Figure S7: Models and calculations for oxygen substitution in WS_2. (a) Normalized pDOS shows that in-gap vacancy states are passivated upon oxygen substitution. (b) Effective charges (Q_{eff}) on surrounding W atoms indicate minimal change in S atom charges, explaining why the S environment remains unaffected while the W spectrum shows an additional high-binding-energy peak. The reference Q_{eff} for pristine W is 1.24. Images have been cropped for clarity and do not represent the whole system used in calculations. Up to 3 S vacancies have been calculated using a $6 \times 6 \times 2$ supercell and $9 \times 9 \times 2$ supercell for 7 O substitution cluster.